Quadrant photodetector sensitivity

Lazo M. Manojlović

Zrenjanin Technical College, Đorđa Stratimirovića 23, 23000 Zrenjanin, Serbia
(lazo.manojlovic@vts-zr.edu.rs)

Received 3 March 2011; revised 30 April 2011; accepted 4 May 2011;
posted 6 May 2011 (Doc. ID 143622); published 5 July 2011

A quantitative theoretical analysis of the quadrant photodetector (QPD) sensitivity in position measurement is presented. The Gaussian light spot irradiance distribution on the QPD surface was assumed to meet most of the real-life applications of this sensor. As the result of the mathematical treatment of the problem, we obtained, in a closed form, the sensitivity function versus the ratio of the light spot $1/e$ radius and the QPD radius. The obtained result is valid for the full range of the ratios. To check the influence of the finite light spot radius on the interaxis cross talk and linearity, we also performed a mathematical analysis to quantitatively measure these types of errors. An optimal range of the ratio of light spot radius and QPD radius has been found to simultaneously achieve low interaxis cross talk and high linearity of the sensor.

OCIS codes: 040.1240, 040.5160, 280.3420, 280.4788.

1. Introduction

Quadrant photodetectors (QPDs) are among the most commonly used position sensitive devices. They enable position and angle measurements with very high precision. Their ability to reach subnanometer resolution for a broad frequency range, the simple signal processing circuitry that follows up every QPD, and a wide operating temperature range make them an optimal solution for position sensing in the nano world. Therefore, QPDs have become irreplaceable parts of many atomic force microscopes, where they are used to sense the microcantilever position [1]. However, the micro and nano worlds are not the only application areas for QPDs. Because they are inherently low noise, highly sensitive, and very robust, QPDs have found, also, a very broad field of applications in the macro world. Lidar [2], laser guided weapons [3], free-space optic communications [4], [5], satellite communications [6], civil [7] and maritime [8] engineering, and the mining industry [9], are just a few possible applications among an unlimited number of them.

Depending on the measuring system requirements, such as resolution, linearity, dynamic range, and frequency bandwidth, between the object whose position is to be measured and the QPD, an optical system consisting of a light source (usually a laser is used) and passive optical components is employed to fulfill the appointed requirements. This optical system has a role in making a relation between the object position and the position of the light spot on the QPD surface. The distribution of the light spot irradiance on the QPD surface mostly depends on the light source used, but also on the object-coupling optics arrangement. Irrespective of the light spot irradiance distribution on the QPD surface, most algorithms for light spot position estimation with respect to the QPD center are based on the position measurement of the light spot's center of gravity. This algorithm enables high sensitivity, high speed, and high resolution position measurement. This problem has been addressed in several papers, in which the measuring system parameters, such as sensitivity, linearity, and resolution, have been calculated and experimentally validated. Probably the best theoretical analysis of the most common case of uniform irradiance distribution is given in [10]. If a laser is used as the light source, then a Gaussian irradiance distribution is usually obtained. A simplified theoretical analysis together with experimental verification of such a position measuring system is given in [11]. Usually, it is assumed that the dimensions

0003-6935/11/203461-09$15.00/0

of the Gaussian-distributed irradiance light spot are much smaller then the QPD dimensions. This implies that the total amount of the irradiated light power enters the QPD surface. However, the above-presented assumption is often not satisfied. In the case where we have long beam paths due to the change of the beam propagation conditions, there can be significant changes of the light spot dimensions on the QPD surface. For example, if we have a servo system that should keep the system movements collinear with the laser beam along a relatively long path, e.g., in civil engineering or the mining industry, then, due to the laser beam divergence, the dimensions of the light spot will fluctuate with respect to the system's movement. Nevertheless, the servo system should stay stable and still keep an acceptable level of system parameters.

The sensitivity of any error sensor in the servo system will greatly influence the overall system working parameters. It was shown that the dimensions of the light spot greatly influence the QPD sensitivity [11,12], irrespective of the irradiance distribution. Therefore, we have theoretically analyzed the influence of the light spot dimension on the QPD sensitivity. In order to match a real system's application conditions, we assumed a Gaussian distribution of the light spot irradiance on the QPD surface. We derive the relation between the QPD sensitivity and the ratio of the $1/e$ light spot radius at the QPD surface and the QPD radius in a closed mathematical form for any possible value of this ratio. This mathematical formula will help the designers of such servo systems match the required system parameters for a certain range of light spot radii. With the increase of the light spot radius with respect to the QPD radius, there will be interaxis cross talk, e.g., a change of the position along one axis will influence the estimated position on the other axis. Therefore, we also analyze the influence of interaxis cross talk on the measurement error and how to minimize it, while maintaining the high linearity of the QPD sensor.

2. Position Measurement

Direct measurements of the light spot position with respect to the QPD center by processing electrical current signals from the QPD are not possible. By measuring these signals, it would be possible to determine only the ratios of positions of the light spot and the QPD's relevant dimensions. To determine these relations, it is essential to know the irradiance distribution on the QPD surface. The exact measurements of these ratios are not possible, and only estimations can be made with the following equations [10,12]:

$$\chi = \frac{(I_{\mathrm{I}} + I_{\mathrm{IV}}) - (I_{\mathrm{II}} + I_{\mathrm{III}})}{(I_{\mathrm{I}} + I_{\mathrm{IV}}) + (I_{\mathrm{II}} + I_{\mathrm{III}})},$$
$$\psi = \frac{(I_{\mathrm{I}} + I_{\mathrm{II}}) - (I_{\mathrm{III}} + I_{\mathrm{IV}})}{(I_{\mathrm{I}} + I_{\mathrm{II}}) + (I_{\mathrm{III}} + I_{\mathrm{IV}})}, \tag{1}$$

where χ and ψ are the estimated values of the ratios along the X and Y axes, respectively, and I_K is the electrical current acquired by the QPD's Kth quadrant, where $K = \mathrm{I}$, II, III, and IV. For these currents, $I_K = \Re P_K$ is valid, where $\Re$ is the photodiode conversion factor, and P_K is the optical power acquired by the QPD's Kth quadrant. Finally, from Eq. (1), the following is obtained for the Y axis:

$$\psi = \frac{(P_{\mathrm{I}} + P_{\mathrm{II}}) - (P_{\mathrm{III}} + P_{\mathrm{IV}})}{(P_{\mathrm{I}} + P_{\mathrm{II}}) + (P_{\mathrm{III}} + P_{\mathrm{IV}})}, \tag{2}$$

where we took only the Y axis due to the symmetry; e.g., everything that is valid for one axis is valid for the other axis if the irradiance distribution is symmetrical with respect to the light spot's center.

3. Sensitivity Analysis

One of the most important parameters that can significantly influence any servo system is the error sensor sensitivity. The sensor sensitivity and the actuator transfer function influence almost equally the dynamic characteristics and stability of every servo system. Therefore, the design of the controller of the servo system is greatly influenced by the sensor sensitivity. In the case where the sensor sensitivity is changed due to a change of the system parameters, it is even more important to know how the sensor sensitivity changes with the change of parameters. As the QPD is used in many critical applications, such as laser-guided weapons for military purposes, for beam alignment in free-space optical communication links, as well as in civil and maritime engineering, where system parameter changes can be significant, it is even more important to figure out in what way the sensor sensitivity will be changed. This will help the designers of such a servo system construct the system in the right way. The QPD is usually used to sense the drift of the laser beam across its surface. In order to achieve the highest possible sensor linearity, single-mode lasers are usually used, and the irradiance distribution on the QPD surface is Gaussian. Because of the long laser beam paths and the different propagation conditions of the laser beam, the change of the light spot radius on the QPD surface can be significant. The relative change of the light spot radius with respect to the QPD radius will strongly influence the sensor sensitivity and, hence, strongly influence the overall system characteristics.

To find the sensitivity of the QPD sensor, we will start our analysis by assuming Gaussian distribution of the irradiance of the light spot falling onto the QPD surface where, for the irradiance distribution $I(r)$, we have:

$$I(r) = \frac{P}{\pi w^2} \exp\left[-\left(\frac{r}{w}\right)^2\right], \tag{3}$$

where r is the radius, P is the overall light source optical power that reaches the QPD surface, and w

is the light spot radius on the QPD surface for which the irradiance drops to the $1/e$ value of its central value. Further, we will assume that the center of the light spot is shifted with respect to the QPD center at the position (x,y). The position of the light spot with respect to the QPD is shown in Fig. 1, where all other relevant geometrical parameters are marked.

First of all, we will find the overall optical power that is captured by the QPD, e.g., the signal obtained as the sum of all powers falling onto each quadrant of the QPD. For the overall optical power $P_\Sigma(x,y)$, we have

$$P_\Sigma(x,y) = P_{\mathrm{I}}(x,y) + P_{\mathrm{II}}(x,y) + P_{\mathrm{III}}(x,y) + P_{\mathrm{IV}}(x,y), \tag{4}$$

where $P_K(x,y)$ (K = I, II, III, and IV) is the optical power captured by the Kth quadrant of the QPD when the light spot center is at the position (x,y) corresponding the QPD center. Instead of finding each optical power that falls on the corresponding quadrant, we will find the overall optical power by integrating the light spot irradiance that is captured by the active QPD surface. In our calculations, we will assume that the dimensions of the gaps between the QPD quadrants are much smaller then QPD radius and light spot radius. By careful analysis of the light spot geometry and by neglecting the gap's influence, we have the following for the overall optical power:

$$P_\Sigma(x,y) = \int_{\theta=0}^{2\pi} \int_{r=0}^{l(x,y,\theta)} I(r) r \cdot \mathrm{d}r \cdot \mathrm{d}\theta, \tag{5}$$

where, for the upper integration limit $l(x,y,\theta)$ is valid,

$$l(x,y,\theta) = \sqrt{R^2 - (x\sin\theta - y\cos\theta)^2} - (x\cos\theta + y\sin\theta), \tag{6}$$

where R is the QPD radius. After partial solving of the integral given in Eq. (5), we have

$$P_\Sigma(x,y) = P\left\{1 - \frac{1}{2\pi}\int_0^{2\pi} \exp\left\{-\left[\frac{l(x,y,\theta)}{w}\right]^2\right\}\mathrm{d}\theta\right\}. \tag{7}$$

For the estimation of the position $\psi(x,y)$ of the light spot center with respect to the QPD center along the Y axis according to Eq. (2), we have

$$\psi(x,y) = \frac{[P_{\mathrm{I}}(x,y) + P_{\mathrm{II}}(x,y)] - [P_{\mathrm{III}}(x,y) + P_{\mathrm{IV}}(x,y)]}{[P_{\mathrm{I}}(x,y) + P_{\mathrm{II}}(x,y)] + [P_{\mathrm{III}}(x,y) + P_{\mathrm{IV}}(x,y)]},$$
$$\psi(x,y) = 2\frac{P_{\mathrm{I}}(x,y) + P_{\mathrm{II}}(x,y)}{P_\Sigma(x,y)} - 1. \tag{8}$$

In order to find the sum of the optical powers $P_{\mathrm{I}}(x,y) + P_{\mathrm{II}}(x,y)$ that fall on the first and the second quadrant, we will use the geometrical representation of the complete QPD geometry given in Fig. 2. According to the geometry that we can see from Fig. 2, for the optical power sum we can write the following:

$$P_{\mathrm{I}}(x,y) + P_{\mathrm{II}}(x,y) = P_{y1}(x,y) + P_{y2}(x,y), \tag{9}$$

where $P_{y1}(x,y)$ is the optical power that is captured by the circle segment limited by the lines $O'A$, $O'B$ and the upper part of the XOY coordinate system, and $P_{y2}(x,y)$ is the optical power that is captured in the triangle $AO'B$.

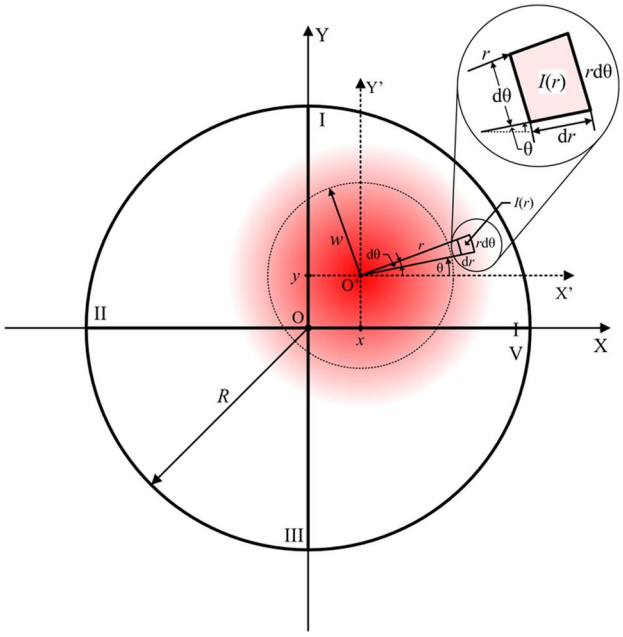

Fig. 1. (Color online) Geometry of the light spot onto the QPD surface with all relevant geometrical parameters.

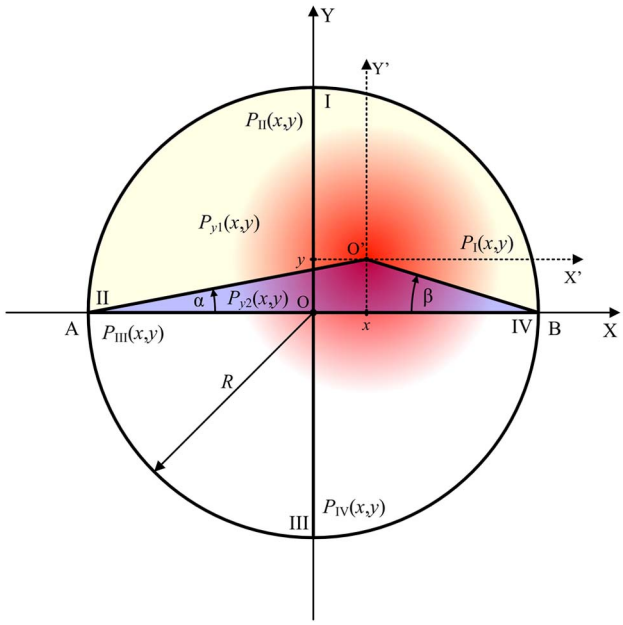

Fig. 2. (Color online) Geometry of the light spot onto the QPD surface that is used for the power sum calculation.

From Eqs. (8) and (9), we have the following:

$$\psi(x,y)=2\frac{P_{y1}(x,y)+P_{y2}(x,y)}{P_{\Sigma}(x,y)}-1=2\frac{P_{y+}(x,y)}{P_{\Sigma}(x,y)}-1, \tag{10}$$

where $P_{y+}(x,y)$ is the optical power that is captured by two upper quadrants. With respect to the geometry shown in Fig. 2 and omitting the gaps influence, we have the following for the optical power $P_{y1}(x,y)$:

$$P_{y1}(x,y)=\frac{P}{\pi w^2}\int_{\theta=-\beta(x,y)}^{\pi+\alpha(x,y)}\int_{r=0}^{l(x,y,\theta)}\exp\left[-\left(\frac{r}{w}\right)^2\right]r\cdot\mathrm{d}r\cdot\mathrm{d}\theta, \tag{11}$$

where $\alpha(x,y)$ is the angle between the line $O'A$ and the X axis and $\beta(x,y)$ is the angle between the line $O'B$ and the X axis for which the following is valid:

$$\alpha(x,y)=\arctan\left(\frac{y}{R-x}\right),$$
$$\beta(x,y)=\arctan\left(\frac{y}{R+x}\right). \tag{12}$$

After combining and rearranging Eqs. (11) and (12), we have

$$P_{y1}(x,y)=\frac{P}{2}\left\{1+\frac{1}{\pi}\left[\arctan\left(\frac{y}{R+x}\right)+\arctan\left(\frac{y}{R-x}\right)\right]-\frac{1}{\pi}\int_{-\beta(x,y)}^{\pi+\alpha(x,y)}\exp\left\{-\left[\frac{l(x,y,\theta)}{w}\right]^2\right\}\mathrm{d}\theta\right\}. \tag{13}$$

Similarly, for the optical power $P_{y2}(x,y)$, we have

$$P_{y2}(x,y)=\frac{P}{\pi w^2}\int_{\theta=\pi+\alpha(x,y)}^{2\pi-\beta(x,y)}\int_{r=0}^{d(x,y,\theta)}\exp\left[-\left(\frac{r}{w}\right)^2\right]r\cdot\mathrm{d}r\cdot\mathrm{d}\theta, \tag{14}$$

where for $d(x,y,\theta)$ we have

$$d(x,y,\theta)=-\frac{y}{\sin\theta}. \tag{15}$$

After combining and rearranging Eqs. (14) and (15), we have

$$P_{y2}(x,y)=\frac{P}{2}\left\{1-\frac{1}{\pi}\left[\arctan\left(\frac{y}{R+x}\right)+\arctan\left(\frac{y}{R-x}\right)\right]-\frac{1}{\pi}\int_{\theta=\pi+\alpha(x,y)}^{2\pi-\beta(x,y)}\exp\left\{-\left[\frac{d(x,y,\theta)}{w}\right]^2\right\}\mathrm{d}\theta\right\}. \tag{16}$$

Finally, for the optical power $P_{y+}(x+y)$ that is captured by two upper quadrants, we have

$$P_{y+}(x,y)=P\left\{1-\frac{1}{2\pi}\int_{-\beta(x,y)}^{\pi+\alpha(x,y)}\exp\left\{-\left[\frac{l(x,y,\theta)}{w}\right]^2\right\}\mathrm{d}\theta-\frac{1}{2\pi}\int_{\theta=\pi+\alpha(x,y)}^{2\pi-\beta(x,y)}\exp\left\{-\left[\frac{d(x,y,\theta)}{w}\right]^2\right\}\mathrm{d}\theta\right\}. \tag{17}$$

For small x and y in comparison with the light spot radius w and the QPD radius R, e.g., $x, y \ll \min(w,R)$, we have

$$\psi(x,y)\approx\frac{\partial\psi(0,0)}{\partial(y/R)}\cdot\left(\frac{y}{R}\right)+\frac{\partial\psi(0,0)}{\partial(x/R)}\cdot\left(\frac{x}{R}\right). \tag{18}$$

Because of the symmetry, the first partial derivative of function $\psi(x,y)$ with respect to the variable x is equal to zero for $x=y=0$, so we have

$$\psi(x,y)\approx\frac{\partial\psi(0,0)}{\partial(y/R)}\cdot\left(\frac{y}{R}\right)=S_y\frac{y}{R}, \tag{19}$$

where S_y is the QPD sensitivity. As can be noticed from the above presented analysis, we defined the sensitivity of the QPD with respect to the relative displacement y/R instead of to the absolute displacement y. The reasons for this are to obtain the QPD sensitivity as a plain number irrespective of the QPD radius or light spot radius and because the QPD radius is the only parameter of the system that does not change with the change of the beam propagation conditions. As we will see later on, such defined QPD sensitivity depends only on the ratio of the light spot radius and the QPD radius. In this case, for the sensitivity, due to the symmetry at the point $x=y=0$, the following is valid:

$$S_y=R\frac{\partial\psi(0,0)}{\partial y}=\frac{2R}{P_{\Sigma}(0,0)}\frac{\partial P_{y+}(0,0)}{\partial y}, \tag{20}$$

where the following is valid,

$$P_{\Sigma}(0,0)=P\left\{1-\exp\left[-\left(\frac{R}{w}\right)^2\right]\right\}. \tag{21}$$

In order to find the QPD sensitivity, we must find the following:

$$\frac{\partial P_{y+}(0,0)}{\partial y}=-\frac{P}{2\pi}\frac{\partial}{\partial y}\left\{\int_{-\beta(x,y)}^{\pi+\alpha(x,y)}\exp\left\{-\left[\frac{l(x,y,\theta)}{w}\right]^2\right\}\mathrm{d}\theta+\int_{\theta=\pi+\alpha(x,y)}^{2\pi-\beta(x,y)}\exp\left\{-\left[\frac{d(x,y,\theta)}{w}\right]^2\right\}\mathrm{d}\theta\right\}\Bigg|_{\substack{x=0\\y=0}}. \tag{22}$$

If we make the following substitutions:

$$A(x,y)=\int_{-\beta(x,y)}^{\pi+\alpha(x,y)}\exp\left\{-\left[\frac{l(x,y,\theta)}{w}\right]^2\right\}\mathrm{d}\theta,$$
$$B(x,y)=\int_{\theta=\pi+\alpha(x,y)}^{2\pi-\beta(x,y)}\exp\left\{-\left[\frac{d(x,y,\theta)}{w}\right]^2\right\}\mathrm{d}\theta, \tag{23}$$

in order to solve the equation given in Eq. (22), we will need to find the first derivatives of both functions given in Eq. (23), e.g., $a=\partial A(0,0)/\partial y$ and $b=\partial B(0,0)/\partial y$. For the parameter a, the following is valid:

$$\begin{aligned}a=&\int_{-\beta(0,0)}^{\pi+\alpha(0,0)}\left\{\frac{\partial}{\partial y}\exp\left\{-\left[\frac{l(x,y,\theta)}{w}\right]^2\right\}\right\}\Bigg|_{\substack{x=0\\y=0}}\mathrm{d}\theta\\&+\exp\left\{-\left\{\frac{l[0,0,\pi+\alpha(0,0)]}{w}\right\}^2\right\}\frac{\partial\alpha(0,0)}{\partial y}\\&+\exp\left\{-\left\{\frac{l[0,0,-\beta(0,0)]}{w}\right\}^2\right\}\frac{\partial\beta(0,0)}{\partial y}.\end{aligned} \tag{24}$$

By calculating the values given in Eq. (24) and by solving the simple integral given in the same equation, this equation becomes

$$a=\frac{2}{R}\left[1+2\left(\frac{R}{w}\right)^2\right]\exp\left[-\left(\frac{R}{w}\right)^2\right]. \tag{25}$$

Further, for parameter b, we have:

$$\begin{aligned}b=&\lim_{y\to0}\left\{\int_{\theta=\pi+\alpha(0,y)}^{2\pi-\beta(0,y)}\frac{\partial}{\partial y}\left\{\exp\left\{-\left[\frac{d(0,y,\theta)}{w}\right]^2\right\}\right\}\mathrm{d}\theta\right.\\&-\exp\left\{-\left\{\frac{d[0,y,2\pi-\beta(0,y)]}{w}\right\}^2\right\}\frac{\partial\beta(0,y)}{\partial y}\\&\left.-\exp\left\{-\left\{\frac{d[0,y,\pi+\alpha(0,y)]}{w}\right\}^2\right\}\frac{\partial\alpha(0,y)}{\partial y}\right\},\end{aligned} \tag{26}$$

where we took the limit of parameter b for $y\to0$ instead of calculating b for $y=0$, because each of the three elements in Eq. (26) has an undefined value in the case of $y=0$. After careful solving of Eq. (26), we have the following:

$$\begin{aligned}b=&-\frac{2}{R}c-\frac{2}{R}\exp\left[-\left(\frac{R}{w}\right)^2\right],\\c=&\lim_{z\to0}\frac{1}{z}\int_z^{\pi-z}\left(\frac{R}{w}\frac{z}{\sin\theta}\right)^2\exp\left[-\left(\frac{R}{w}\frac{z}{\sin\theta}\right)^2\right]\mathrm{d}\theta.\end{aligned} \tag{27}$$

The parameter c is given with the limit of the integral as shown in Eq. (27). The closed form solution for the parameter c exists, but the calculation of this parameter is rather complicated and not straightforward, so the solution of this limit of the integral is given in Appendix A, where we obtained

$$c=\sqrt{\pi}\frac{R}{w}\mathrm{erf}\left(\frac{R}{w}\right), \tag{28}$$

where $\mathrm{erf}(\bullet)$ is the error function of its argument, so, finally, for parameter b we have

$$b=-2\sqrt{\pi}\frac{1}{w}\mathrm{erf}\left(\frac{R}{w}\right)-\frac{2}{R}\exp\left[-\left(\frac{R}{w}\right)^2\right]. \tag{29}$$

At the end we have the following:

$$\begin{aligned}\frac{\partial P_{y+}(0,0)}{\partial y}&=-\frac{P}{2\pi}(a+b)\\&=\frac{P}{\pi R}\frac{R}{w}\left\{\sqrt{\pi}\mathrm{erf}\left(\frac{R}{w}\right)-\frac{2R}{w}\exp\left[-\left(\frac{R}{w}\right)^2\right]\right\},\end{aligned} \tag{30}$$

and, finally, for the QPD sensitivity we have

$$S_y=\frac{2}{\sqrt{\pi}}\frac{R}{w}\frac{\mathrm{erf}\left(\frac{R}{w}\right)\exp\left[\left(\frac{R}{w}\right)^2\right]-\frac{2}{\sqrt{\pi}}\frac{R}{w}}{\exp\left[\left(\frac{R}{w}\right)^2\right]-1}. \tag{31}$$

As can be seen from Eq. (31), we obtained the QPD sensitivity in the case of a circular QPD and Gaussian distribution of the light spot irradiance onto the QPD surface in the closed form. In order to see how the QPD sensitivity is changed with respect to the light spot radius, we plot the diagram of the QPD sensitivity S_x and S_y (due to the light spot and QPD symmetry, the sensitivity along the X axis, S_x, and the Y axis, S_y, are identical, e.g., $S_x=S_y$) versus the ratio of the light spot radius and QPD radius w/R. This diagram is presented in Fig. 3. By analyzing Fig. 3, one can notice two separate behaviors of the sensitivity function given in Eq. (31). For small values of ratio w/R ($w/R<1$) the QPD sensitivity decreases with the increase of the light spot radius with the approximate rate of 20 dB/decade, whereas, for large values of ratio w/R ($w/R>1$), the QPD sensitivity decreases with the increase of the light spot radius with the approximate rate of 40 dB/decade.

Besides the significant change of the light spot radius onto the QPD surface due to the significant changes of the beam propagation conditions, which generally occur on a relatively long time scale, there also occur rather smaller but faster changes of the light spot radius due to some abrupt changes of the system configuration or externally induced vibration. In the former case, the small changes of the light spot radius will induce change of the QPD sensitivity, which, on the other hand, can influence the overall servo system. Therefore, it would be interesting to see how the relative change of the QPD sensitivity is changed with respect to the relative change of the light spot radius. Taking into consideration the above-mentioned analysis, we will find the absolute change ΔS_y of the QPD sensitivity

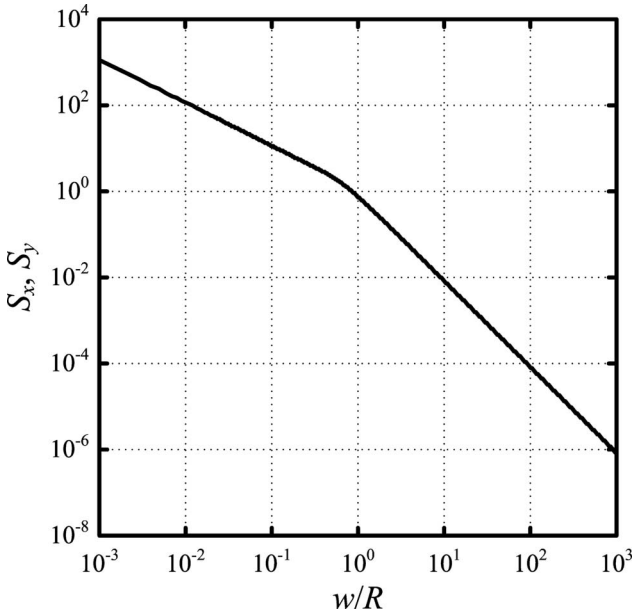

Fig. 3. QPD sensitivity S_x and S_y versus the ratio of light spot radius and QPD radius w/R.

versus the absolute change of the light spot radius Δw. According to Eq. (31), we have

$$\Delta S_y = \frac{dS_y}{dw}\Delta w = -\frac{R}{w^2}\frac{dS_y}{d\left(\frac{R}{w}\right)}\Delta w. \tag{32}$$

We are interested in the relative change $\Delta S_y/S_y$ of the QPD sensitivity versus the relative change $\Delta w/w$ of the light spot radius, so according to Eqs. (31) and (32), we have

$$\frac{\frac{\Delta S_y}{S_y}}{\frac{\Delta w}{w}} = -1 - 2\left(\frac{R}{w}\right)^2\left\{\frac{1}{\exp\left[\left(\frac{R}{w}\right)^2\right]-1} + \frac{\frac{2}{\sqrt{\pi}}\frac{R}{w}}{\operatorname{erf}\left(\frac{R}{w}\right)\exp\left[\left(\frac{R}{w}\right)^2\right]-\frac{2}{\sqrt{\pi}}\frac{R}{w}}\right\}. \tag{33}$$

The ratio of the QPD sensitivity relative change and the light spot radius relative change versus the ratio of light spot radius and QPD radius is given in Fig. 4.

If we analyze the diagram given in Fig. 4, we can notice an abrupt increase in the absolute value of the ratio of the QPD sensitivity relative change and the light spot radius relative change with respect to the ratio of light spot radius and QPD radius. This abrupt change occurs when the light spot radius approaches the QPD radius.

4. Interaxis Cross Talk

One of the problems that can occur during the application of QPD sensors is interaxis cross talk. The nonuniformity of the light spot irradiance distribution on the QPD surface will cause the change of the estimated position of the light spot center in one axis as the position of the light spot center shifts along the other axis. If the shift in the orthogonal axis is much bigger than the shift in the axis where the position of the light spot center is being measured, we can have a large measurement error. Therefore, it would be interesting to make the Taylor expansion of the function $\psi(x,y)$ around the point $x = y = 0$ and to make a third-order approximation of the function $\psi(x,y)$. If we make the expansion of this function and if we take into account the symmetry of this function, we can write

$$\psi(x,y) \approx S_y\left(\frac{y}{R}\right)\left\{1 + \frac{1}{S_y}\left[S_{yyy}\left(\frac{y}{R}\right)^2 + S_{yxx}\left(\frac{x}{R}\right)^2\right]\right\}, \tag{34}$$

where S_{yyy} and S_{yxx} are the third-order coefficients and where we neglect higher-order elements. For these coefficients we have the following:

$$S_{yyy} = \frac{1}{6}R^3\frac{\partial^3\psi(0,0)}{\partial y^3}, \qquad S_{yxx} = \frac{1}{2}R^3\frac{\partial^3\psi(0,0)}{\partial y\partial x^2}. \tag{35}$$

The derivation of these coefficients is very complicated and time consuming, but, from the mathematical point of view, not so challenging. The only mathematically challenging task is to solve the same limit of the integral as it is given in Eq. (27) and solved in the Appendix A. For this reason, the derivation of these coefficients is omitted in this paper and only the final solutions are presented. For these final solutions we have

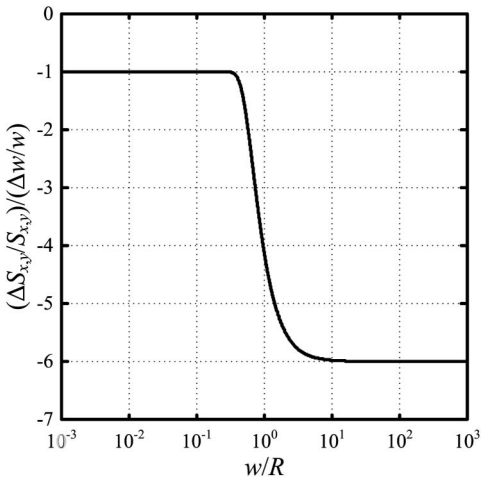

Fig. 4. Ratio of the QPD sensitivity relative change and the light spot radius relative change versus the ratio of light spot radius and QPD radius.

$$S_{yyy} = \frac{2}{3\pi}\frac{p+q}{\exp\left[\left(\frac{R}{w}\right)^2\right]-1},$$

$$p = 2 + 3\left(\frac{R}{w}\right)^2 + \frac{4}{3}\left(\frac{R}{w}\right)^6 - \frac{4\left(\frac{R}{w}\right)^2}{\exp\left[\left(\frac{R}{w}\right)^2\right]-1},$$

$$q = \frac{2\sqrt{\pi}\left(\frac{R}{w}\right)\operatorname{erf}\left(\frac{R}{w}\right)}{1-\exp\left[-\left(\frac{R}{w}\right)^2\right]} - 3\sqrt{\pi}\left(\frac{R}{w}\right)^2\operatorname{erf}\left(\frac{R}{w}\right)\exp\left[\left(\frac{R}{w}\right)^2\right], \quad (36)$$

$$S_{yxx} = \frac{2}{3\pi}\frac{3+5\left(\frac{R}{w}\right)^2+10\left(\frac{R}{w}\right)^4-2\left(\frac{R}{w}\right)^6}{\exp\left[\left(\frac{R}{w}\right)^2\right]-1}. \quad (37)$$

In order to check the behavior of these coefficients, the dependence of these coefficients on the ratio w/R is presented in Fig. 5. As can be seen from diagrams presented in Fig. 5, in the case of S_{yxx} (line 1) for very small values of the ratio w/R, we have almost no influence of the light spot center movement along the X axis on the measurement of the light spot position along the Y axis. This is expected because the complete optical power is captured by the QPD, so the movement in one axis will not influence the position measurement in the other axis and, hence, there will be no interaxis cross talk. The much bigger problem for the small values of the parameter w/R is the relatively high value of the S_{yyy} (line 2) parameter, which will significantly deteriorate the linearity of the measurement. In order to reduce the measurement nonlinearity, we need to increase the w/R parameter. However, this will, on the other hand, increase the interaxis cross talk. Nevertheless, the good news concerning the interaxis cross talk is that, as can be seen from the upper inset in Fig. 5, the parameter S_{yxx} has zero value for $w/R = 0.426$. This means that, for this parameter value, we will have almost no interaxis cross talk. There can be some influences of the higher-order (higher than third order) elements of the Taylor expansions of the function $\psi(x,y)$, but they are much smaller than the influence of the third-order elements (S_{yxx}), especially from small values of x and y. In this way, by choosing $w/R = 0.426$, we keep the interaxis cross talk very small while still keeping the nonlinearity at the acceptable level. If we need to design the QPD sensor in such a way to suppress the nonlinearity as much as possible, we need to set $w/R = 1.15$ in order to have the lowest possible nonlinearity for a relatively large range of x and y values. From the lower inset in Fig. 5, one can see that, for $w/R = 1.15$, parameter S_{yyy} has zero value, meaning the lowest nonlinearity of the QPD sensor. Of course, there will be influences of the higher-order (higher than third order) elements of the Taylor expansions of the function $\psi(x,y)$, but they are much smaller than the influence of the third-order elements (S_{yyy}).

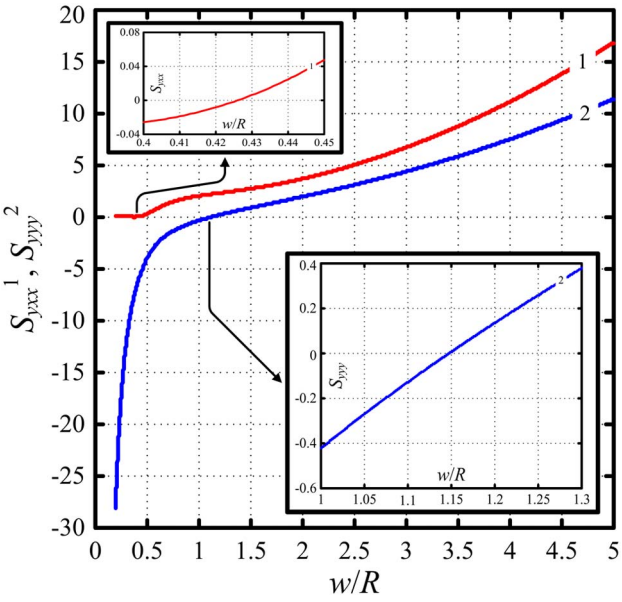

Fig. 5. (Color online) Coefficients S_{yyy} (line 1) and S_{yyx} (line 2) versus the ratio w/R.

Bearing in mind all that is presented above and by careful inspection of Fig. 5, one can conclude that, concerning the overall parameters of the QPD sensor, the best choice for the parameter w/R is somewhere in the range $0.5 < w/R < 1.5$. This range of the parameter w/R will, at the same time, provide low nonlinearity and low interaxis cross talk of the QPD sensor, thus meeting the requirements of most measuring and servo systems.

5. Conclusion

A theoretical analysis of the QPD sensitivity, where a Gaussian distribution of the light spot irradiance is assumed, is presented. The sensitivity was calculated for the full range of the ratio between the light spot radius and the QPD radius. In order to obtain a closed form solution of the sensitivity function, a relatively complicated mathematical analysis was performed. The obtained solution shows different behavior of the sensitivity function from small and large ratios of the light spot radius and the QPD radius. For this ratio smaller than unity, the QPD sensitivity decreases with the increase of the light spot radius with the approximate rate of 20 dB/decade, where, for a ratio larger than unity, the QPD sensitivity decreases with the increase of the light spot radius with the approximate rate of 40 dB/decade.

As the interaxis cross talk can be a significant source of error, we performed, also, a theoretical analysis of the influence of the light spot center movement on the position measurement along the

orthogonal axis. The analysis shows that, in order to simultaneously maintain low interaxis cross talk and high linearity of the QPD sensor, the ratio of the light spot radius and the QPD radius should be in the range between 0.5 and 1.5.

Appendix A

In this Appendix, the solution in the closed form of the limit of the integral given in Eq. (27) is presented. For this limit of the integral we have the following:

$$c = \lim_{z\to 0}\frac{1}{z}\int_z^{\pi-z}\left(\frac{R}{w}\frac{z}{\sin\theta}\right)^2\exp\left[-\left(\frac{R}{w}\frac{z}{\sin\theta}\right)^2\right]\mathrm{d}\theta. \quad \text{(A1)}$$

As the limit in Eq. (A1) has the form of "0/0," in order to find the limit value of this expression, we need to apply the l'Hôpital rule, so, for the parameter c, we can write

$$c = \lim_{z\to 0}\frac{d}{dz}\left\{\int_z^{\pi-z}\left(\frac{R}{w}\frac{z}{\sin\theta}\right)^2\exp\left[-\left(\frac{R}{w}\frac{z}{\sin\theta}\right)^2\right]\mathrm{d}\theta\right\}. \quad \text{(A2)}$$

After the differentiation in Eq. (A2), we have

$$\begin{aligned} c &= 2\left(\frac{R}{w}\right)^2\exp\left[-\left(\frac{R}{w}\right)^2\right] + 2c_1,\\ c_1 &= \lim_{z\to 0}\frac{1}{z}\int_z^{\pi-z}\left(\frac{R}{w}\frac{z}{\sin\theta}\right)^4\exp\left[-\left(\frac{R}{w}\frac{z}{\sin\theta}\right)^2\right]\mathrm{d}\theta. \end{aligned} \quad \text{(A3)}$$

The parameter c_1 has also the form of "0/0," so, in order to find the limit value of this expression, we need to apply once again the l'Hôpital rule. Therefore, for the parameter c_1 we can write

$$\begin{aligned} c_1 &= \frac{2}{3}\left(\frac{R}{w}\right)^4\exp\left[-\left(\frac{R}{w}\right)^2\right] + \frac{2}{3}c_2,\\ c_2 &= \lim_{z\to 0}\frac{1}{z}\int_z^{\pi-z}\left(\frac{R}{w}\frac{z}{\sin\theta}\right)^6\exp\left[-\left(\frac{R}{w}\frac{z}{\sin\theta}\right)^2\right]\mathrm{d}\theta. \end{aligned} \quad \text{(A4)}$$

In a similar way, for the parameter c_2, we can write the following:

$$\begin{aligned} c_2 &= \frac{2}{5}\left(\frac{R}{w}\right)^6\exp\left[-\left(\frac{R}{w}\right)^2\right] + \frac{2}{5}c_3,\\ c_3 &= \lim_{z\to 0}\frac{1}{z}\int_z^{\pi-z}\left(\frac{R}{w}\frac{z}{\sin\theta}\right)^8\exp\left[-\left(\frac{R}{w}\frac{z}{\sin\theta}\right)^2\right]\mathrm{d}\theta. \end{aligned} \quad \text{(A5)}$$

According to Eqs. (A3)–(A5), we can generalize the relation between the coefficients c_n and c_{n+1}:

$$c_n = \frac{2}{2n+1}\left(\frac{R}{w}\right)^{2n+2}\exp\left[-\left(\frac{R}{w}\right)^2\right] + \frac{2}{2n+1}c_{n+1}, \quad \text{(A6)}$$

which can easily be proved by using the mathematical induction method. Therefore, according to Eqs. (A1) and (A6), we have

$$\begin{aligned} c &= 2s^2\exp(-s^2)\sum_{k=0}^{+\infty}\frac{(2s^2)^k}{\prod_{j=0}^{k}(2j+1)} + \lim_{k\to+\infty}a_k,\\ s &= \frac{R}{w}, \qquad a_k = \frac{2^{k+1}}{1\cdot 3\cdot\ldots\cdot(2k+1)}c_k,\\ c_k &= \lim_{z\to 0}\frac{1}{z}\int_z^{\pi-z}\left(\frac{sz}{\sin\theta}\right)^{2(k+1)}\exp\left[-\left(\frac{sz}{\sin\theta}\right)^2\right]\mathrm{d}\theta. \end{aligned} \quad \text{(A7)}$$

Now we should prove that a_k tends to zero when k tends to infinity. In order to prove this, we will observe the following:

$$\lim_{k\to+\infty}\frac{a_{k+1}}{a_k} = \lim_{k\to+\infty}\frac{2}{2k+3}\frac{c_{k+1}}{c_k}. \quad \text{(A8)}$$

If we combine Eqs. (A7) and (A8) and as the limit values in the nominator c_{k+1} and in the denominator c_k both tend in the same manner (parameter z tends to zero for both of them simultaneously), we can unify both of the limit values in one, and so we have

$$\lim_{k\to+\infty}\frac{a_{k+1}}{a_k} = 2\lim_{k\to+\infty}\frac{\lim_{z\to 0}\frac{\int_z^{\pi-z}\left(\frac{sz}{\sin\theta}\right)^{2(k+2)}\exp\left[-\left(\frac{sz}{\sin\theta}\right)^2\right]\mathrm{d}\theta}{\int_z^{\pi-z}\left(\frac{sz}{\sin\theta}\right)^{2(k+1)}\exp\left[-\left(\frac{sz}{\sin\theta}\right)^2\right]\mathrm{d}\theta}}{2k+3}. \quad \text{(A9)}$$

From Eq. (A9), one can notice that $\theta\in[z,\pi-z]$, where $z\to 0$, so we have the following condition fulfilled: $z/\sin\theta\le 1$. Therefore, (A9) becomes

$$\lim_{k\to+\infty}\frac{a_{k+1}}{a_k} \le 2s^2\lim_{k\to+\infty}\frac{1}{2k+3} = 0. \quad \text{(A10)}$$

On the other hand, we have, according to Eqs. (A7) and (A8) that $a_{k+1}/a_k \ge 0$, so, finally, we have

$$\lim_{k\to+\infty}\frac{a_{k+1}}{a_k} = 0. \quad \text{(A11)}$$

According to the d'Alembert criterion and Eq. (A11), the series a_k converges, so we can write

$$\lim_{k\to+\infty}a_k = 0, \quad \text{(A12)}$$

where, in this case, from Eqs. (A7) and (A12) we have

$$c = 2s^2 \exp(-s^2) f(s), \qquad f(s) = \sum_{k=0}^{+\infty} \frac{\left(\sqrt{2}\, s\right)^{2k}}{\prod_{j=0}^{k} (2j+1)}. \tag{A13}$$

Further, after multiplying both sides of the lower equation in Eq. (A13) with $\sqrt{2}s$, we have

$$u f(u) = \sum_{k=0}^{+\infty} \frac{u^{2k+1}}{\prod_{j=0}^{k} (2j+1)}, \tag{A14}$$

where we make the following substitution: $u = \sqrt{2}s$. If we derivate both sides of the equation given in Eq. (A14) with respect to the variable u, we obtain

$$f(u) + u\dot{f}(u) = 1 + u^2 f(u), \tag{A15}$$

where $\dot{f}(u) = df(u)/du$. The differential equation given in Eq. (A15) can be rearranged in the following way:

$$\dot{f}(u) + \left(\frac{1}{u} - u\right) f(u) = \frac{1}{u}. \tag{A16}$$

The differential equation given in Eq. (A16) is the first-order nonhomogeneous linear differential equation. The solution of this differential equation is given as

$$f(s) = \frac{1}{\sqrt{2}s} \exp(s^2) \left[C + \sqrt{2} \int \exp(-s^2) \mathrm{d}s \right], \tag{A17}$$

where we make, again, the following substitution: $s = u/\sqrt{2}$, and C is an arbitrary constant that depends only on the initial conditions. With respect to this, Eq. (A17) becomes

$$f(s) = \frac{1}{\sqrt{2}s} \exp(s^2) \left[C + \sqrt{2} \int_0^s \exp(-t^2) \mathrm{d}t \right], \tag{A18}$$

so Eq. (A18) can be written as

$$f(s) = \frac{1}{\sqrt{2}s} \exp(s^2) \left[C + \sqrt{\frac{\pi}{2}} \mathrm{erf}(s) \right]. \tag{A19}$$

Constant C can be found from Eq. (A13), where we have $f(s=0) = 1$. Function $f(s)$, given in Eq. (A19), has an undefined value for $s = 0$, but if we let $s \to 0$, then $\lim_{s\to 0} f(s) = 1$ must be satisfied in order to have an equivalency between both representations of the same function. Therefore, $C = 0$ must be fulfilled, so we have

$$f(s) = \frac{\sqrt{\pi}}{2} \frac{\exp(s^2)}{s} \mathrm{erf}(s). \tag{A20}$$

By combining Eqs. (A13) and (A20), we obtain

$$c = \sqrt{\pi} s \cdot \mathrm{erf}(s). \tag{A21}$$

Finally, if we take again the substitution that we made earlier, e.g., $s = R/w$, we obtain Eq. (28).

This work has been fully supported by the Serbian Academy of Science and Arts under project Infrared and Laser Techniques.

References

1. B. Bhushan, *Scanning Probe Microscopy in Nanoscience and Nanotechnology* (Springer-Verlag, 2010).
2. A. Mäkynen, J. Kostamovaara, and R. Myllylä, "Laser-radar-based three dimensional sensor for teaching robot paths," Opt. Eng. **34**, 2596–2602 (1995).
3. G. Marola, D. Santerini, and G. Prati, "Stability analysis of direct-detection cooperative optical beam tracking," IEEE Trans. Aerosp. Electron. Syst. **25**, 325–333 (1989).
4. C. G. Boisset, "Design and construction of an active alignment demonstrator for a free-space optical interconnect," IEEE Photon. Technol. Lett. **7**, 676–678 (1995).
5. F. Wu, L. VJ, M. S. Islam, D. A. Horsley, R. G. Walmsley, S. Mathai, D. Houng, M. R. T. Tan, and S.-Y. Wang, "Integrated receiver architectures for board-to-board free-space optical interconnects," Appl. Phys. A **95**, 1079–1088 (2009).
6. M. Toyoda, K. Araki, and Y. Suzuki, "Measurement of the characteristics of a quadrant avalanche photodiode and its application to a laser tracking system," Opt. Eng. **41**, 145–149 (2002).
7. H. Wenzel, *Health Monitoring of Bridges* (Wiley, 2009).
8. A. Mäkynen, J. Kostamovaara, and R. Myllylä, "Tracking laser radar for 3-D shape measurements of large industrial objects based on time-of-flight laser rangefinding and position-sensitive detection techniques," IEEE Trans. Instrum. Meas. **43**, 40–49 (1994).
9. R. Herteau, M. St-Amant, Y. Laperriere, and G. Chevrette, "Optical guidance system for underground mine vehicles," in *IEEE International Conference on Robotics and Automation* (IEEE, 1992), pp. 639–644.
10. L. G. Kazovsky, "Theory of tracking accuracy of laser systems," Opt. Eng. **22**, 339–347 (1983).
11. E. J. Lee, Y. Park, C. S. Kim, and T. Kouh, "Detection sensitivity of the optical beam deflection method characterized with the optical spot size on the detector," Curr. Appl. Phys. **10**, 834–837 (2010).
12. L. M. Manojlovic and Z. P. Barbaric, "Optimization of optical receiver parameters for pulsed laser-tracking systems," IEEE Trans. Instrum. Meas. **58**, 681–690 (2009).